RESEARCH ARTICLE

Effects of Differential Distribution of Microvessel Density, Possibly Regulated by miR-374a, on Breast Cancer Prognosis

Jian-Yi Li, Yang Zhang, Wen-Hai Zhang*, Shi Jia, Ye Kang, Rui Tian

Abstract

Background: The discovery that microRNAs (miRNAs) regulate proliferation, invasion and metastasis provides a principal molecular basis of tumor heterogeneity. Microvessel distribution is an important characteristic of solid tumors, with significant hypoxia occurring in the center of tumors with low blood flow. The distribution of miR-374a in breast tumors was examined as a factor likely to be important in breast cancer progression. Methods: Breast tissue samples from 40 patients with breast cancer were classified into two groups: a highly invasive and metastatic group (HIMG) and a low-invasive and metastatic Group (LIMG). Samples were collected from the center and edge of each tumor. In each group, six specimens were examined by microRNA array, and the remaining 14 specimens were used for real-time RT-qPCR, Western blot and immunohistochemical analyses. Correlation analysis was performed for the miRNAs and target proteins. Follow-up was carried out during 28 months to 68 months after surgery, and survival data were analyzed. Results: In the LIMG, the relative content of miR-374a was lower in the center of the tumor than at its edge; in the HIMG, it was lower at the edge of the tumor, and miR-374a levels were lower in breast cancer tissues than in normal tissues. There was no difference between VEGF-A and VCAM-1 mRNA levels at the edge and center of the tumor; however, we observed a significant difference between VEGF-A and VCAM-1 protein expression levels in these two regions. There was a negative correlation between miR-374a and target protein levels. The microvessel density (MVD) was lower in the center of the tumor than at its edge in HIMG, but the LIMG vessels were uniformly distributed. There was a significant positive correlation between MVD and the number of lymph node metastases (Pearson correlation, r=0.912, *P*<0.01). The median follow-up time was 48.5 months. LIMG had higher rate of disease-free survival (100%, *P*=0.013) and longer median survival time (66 months) than HIMG, which had a lower rate of 75% and shorter median survival time (54 months). Conclusions: Our data demonstrated miR-374a to be differentially distributed in breast cancer; VEGF-A and VCAM-1 mRNA had coincident distribution, and the distribution of teh respective proteins was uneven and opposite to that for the miR-374a. These data might explain the differences in the distribution of MVD in breast cancer and variation in breast cancer prognosis.

Keywords: Breast cancer - miR-374a - VEGF-A - vascular cell adhesion molecule-1 - microvessel density

Asian Pacific J Cancer Prev, **14 (3)**, 1715-1720

Introduction

Solid tumors cannot develop beyond the size of 1–2mm without the induction of angiogenesis, which is regulated by natural inhibitors (Jakóbisiak et al., 2003). Angiogenesis is critical for tumor growth and thus presents a promising therapeutic target (Mackey et al., 2012). Interestingly, the solid tumors are not homogeneous; one of the main characteristics of solid tumors is their heterogeneous microvessel distribution, with significant hypoxia occurring in the central regions with a low blood flow (Balsat et al., 2011). MicroRNAs (miRNAs) are a class of endogenous, small, non-coding RNAs that control gene expression by interacting with target mRNAs, causing either mRNA degradation or translational repression (Pritchard et al., 2012). There is increasing evidence that miRNAs play important roles in cancer progress as well as in angiogenesis (Caporali et al., 2011). The distribution of miRNAs in breast tumors might be an important factor in breast cancer progress, and as such, it is worth examining in some detail. In this study, we found that miR-374a was differentially distributed in breast cancer; VEGF-A and VCAM-1 mRNA had coincident distribution, and the distribution of VEGF-A and VCAM-1 proteins was uneven and opposite to that for the miR-374a. These data might explain the differences in the distribution of MVD in breast cancer and the differences in breast cancer prognoses.

Materials and Methods

Patients and groups

Forty human breast tumor samples were obtained by surgical resection from patients treated at Shengjing

*Department of Breast Surgery, Shengjing Hospital of China Medical University, Shenyang, Liaoning, China *For correspondence: sjbreast@sina.com, zhangwh@sj-hospital.org*

Hospital of China Medical University (SJHCMU) from 2005 to 2009. Inclusion criteria were: invasive ductal carcinoma, stage II, no history of neo-adjuvant therapy and radiotherapy, no family history of other cancers, and no accessory breast cancer. From this rather homogeneous and relatively small group of patients, we collected anthropometric data (age at diagnosis, menopause, chemotherapy, radiotherapy, hormonal therapy), as well as the parameters of the tumor (size, location, histological grade, lymphovascular invasion, immunohistochemical indications). Pathological tumor stage was assessed according to the criteria described in the 6th edition of the American Joint Committee on Cancer (AJCC) staging manual. The tumors were classified into histological grades I–III according to the Nottingham combined histological grading system. Twenty patients fulfilled the criteria for the HIMG. The patient characteristics in this group were: lymph node metastases, histological grade III; they were Her2-positive, vascular cancer embolus-positive, estrogen and progesterone receptor-negative, p53-positive, and had Ki67 index greater than or equal to 14%. Other twenty patients were categorized as the LIMG; these patients had no lymph node metastases or micro-metastases, their tumors were of histological grade I, they were Her2-negative, vascular cancer embolus-negative, estrogen and progesterone receptor-positive, p53-negative, and had Ki67 index smaller than 14% (Table 1).

We randomly chose 20 patients with benign tumors and normal breast tissues for the control group. All patients gave informed consent and signed the Informed Consent Sheet. Each group of 20 specimens was randomly divided into two sections: the first section of six samples for microRNA array screenings, and the second section of 14 samples to be used for validation experiments by real-time RT-qPCR, Western blot analyses and immunohistochemical analyses.

All patients received adjuvant systemic therapy (chemotherapy, radiotherapy, and endocrine therapy) guided by the National Comprehensive Cancer Network (NCCN). Follow-up was carried out at 3-month intervals during the first two years, at 6-month intervals during the next three years, and at 12-month intervals thereafter. The follow-up ended in June 2012. The diagnosis of local recurrence and contralateral breast cancer was achieved by biopsy, and distant metastasis was diagnosed by more than two types of imaging examinations. The outcome criteria were relapse and death due to disease, time until progression (disease-free survival, DFS), and overall survival (OS).

The study was approved by the Ethics Committee of Shengjing Hospital.

Tumor samples

The largest section of the tumor, which was parallel to the chest wall and more than 3 mm thick, was obtained by open surgery. The center and edge of the tumor were determined by eye, and the weight of each specimen was more than 30 mg (Figure 1). Similar quantities of normal breast tissue were obtained from patients in the control group. All samples were stored at -80 °C after quick freezing in liquid nitrogen.

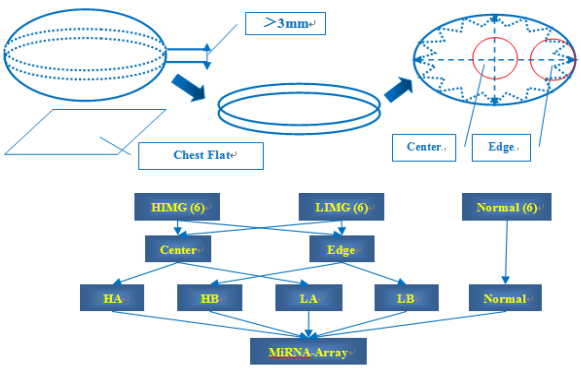

Figure 1. Diagram of Tumor Partition and Specimen Mix

Table 1. Grouping Criteria

Grouped Criteria	Low invasive and metastatic group	High invasive and metastatic group
Lymph Nodes Metastasis by HE	No	Yes
Micro-Metastasis by CK-22	No	Unnecessary
Histological Grading	I	III
Tumor Embolus	Negative	Positive
Her2 receptor Status	Negative	Positive
ER & PR	Positive	Negative
P53	Negative	Positive
Ki67	<14%	≥14%

Illustration: All indicators of immunohistochemical staining need to meet verification of two pathological diagnosis centers

MicroRNA array

For each group of six randomly selected samples, the center and edge fragments of the tumor were mixed with a similar sample from the control group; five such mixed samples (the central part of HIMG - HA, the edge part of HIMG - HB, the central part of LIMG - LA, the edge part of LIMG - LB, and Normal) were screened using microRNA arrays (Figure 2). The 6th generation miRCURYTM LNA Array (v.16.0) (Exiqon; Vedbaek, Denmari) contains more than 1891 capture probes, covering all human, mouse and rat microRNAs annotated in miRBase 16.0, as well as all viral microRNAs related to these species. In addition, this array contains capture probes for 66 new miRPlus™ human microRNAs. Total RNA was isolated using TRIzol (Invitrogen; Carlsbad, CA, USA) and the miRNeasy Mini Kit (QIAGEN, Spoorstraat, Netherlands) according to the manufacturer's instructions, obtaining all RNA species, including miRNAs. RNA quality and quantity were measured using a nanodrop spectrophotometer (ND-1000, Nanodrop Technologies, Wilmington, USA) and RNA integrity was determined by gel electrophoresis. After RNA isolation from the samples, the miRCURY™ Hy3™ /Hy5™ Power labeling kit (Exiqon) was used according to the manufacturer's guidelines for miRNA labeling. One microgram of each sample was 3'-end-labeled with Hy3TM fluorescent label, using T4 RNA ligase according to the procedure described below. RNA in 2.0 μl of water was combined with 1.0 μl CIP buffer and CIP (Exiqon). The mixture was incubated for 30 min at 37°C, and was terminated by incubation for 5 min at 95°C. Then, 3.0 μl of labeling buffer, 1.5 μl of fluorescent label (Hy3TM), 2.0 μl of DMSO, and 2.0 μl of labeling enzyme were added to the mixture. The labeling

reaction was incubated for 1 h at 16 °C, and terminated by incubation for 15 min at 65 °C. The Hy3TM-labeled samples were hybridized on the miRCURYTM LNA Array (v.16.0) (Exiqon) according to the instructions in the array manual. The mixture of 25 μl of Hy3TM-labeled samples and 25 μl hybridization buffer were denatured for 2 min at 95 °C, incubated on ice for 2 min, and then hybridized to the microarray for 16–20 h at 56 °C in the 12-Bay Hybridization System (Hybridization System-Nimblegen Systems, Inc., Madison, WI, USA), which provides an active mixed action and constant incubation temperature to improve hybridization uniformity and enhance signals. Following hybridization, the slides were washed several times with wash buffer from the Exiqon kit, and finally dried by centrifugation for 5 min at 400 rpm. The slides were then scanned using Axon GenePix 4000B microarray scanner (Axon Instruments; Foster City, CA). Scanned images were imported into GenePix Pro 6.0 system (Axon Instruments) for grid alignment and data extraction. Replicated miRNAs were averaged and miRNAs with intensities ≥50 in all samples were chosen for calculating the normalization factor. Expressed data were normalized using median normalization. After normalization, differentially expressed miRNAs were identified through fold-change filtering. Hierarchical clustering was performed using Multiple Experiment Viewer (MEV) software (v4.6, TIGR).

Real-time qRT-PCR

Small RNA and total RNA from the breast tissue were extracted using the mirVana™ miRNA Isolation Kit (AM1560, ABI, USA). Reverse transcription was performed with the PrimeScript® RT reagent kit (DRR037A, Takara, Japan) in a final volume of 10 μl containing 200 ng RNA and other reagents, according to the protocol. Poly-A tail was added to the small RNA by poly-A polymerase (NEB, M0276) before reverse transcription using primers (U6 F: CTCGCTTCGGCAGCACA, R: AACGCTTCACGAATTTGCGT; miR-374a F: TTATA ATACAACCTGATAAGTG, R: TGTCAACGATACGC TACGTAA; VEGF-A F: CAACTTCTGGGCTGTTCT, R: TCTCCTCTTCCTTCTCTTCT; VCAM-1 F: GAACCC AAACAGAGGCAGAG, R: GGTATCCCATCACTTGA GCAG; GAPDH F: GGTGAAGGTCGGAGTCAACG, R: CCATGTAGTTGAGGTCAATGAAG). Real-time quantitative PCR was performed on the Roche Light Cycler 2.0 with SYBR® Premix Ex Taq™ (Takara, DRR041A). For each sample, real-time PCR was performed in a final volume of 10 μl containing PCR master mix, 50 ng genomic DNA or 5 ng cDNA, and primers (250 nM). For the negative control, the template was replaced with purified non-reverse-transcribed RNA. Each experiment was done in triplicate. Average GAPDH Ct values were subtracted from each average Ct value of interest to give ΔCt.

Western blot analysis

Protein extracts, SDS-PAGE, electrotransfer and immunoblotting were performed according to standard procedures. VEGF-A and VCAM-1 expression were detected by antibody sc-6836 (Santa Cruz, USA), raised against the C-terminal of VEGF-A and VCAM-1. A GAPDH antibody was used as an internal control (KC-5G4, Kangchen Biotech, China). Densitometric analysis was done using Quantity One (version 4.5, Bio-Rad, USA).

MVD evaluation by IHC staining

MVD was evaluated by immunohistochemical staining of tumor vessels for CD34 in whole tissue sections. Any immunopositive single cell or cluster of cells, clearly separated from adjacent clusters and from the background, with or without a lumen, was considered to be an individual vessel. Microvessels in the five most vascularized areas in a 200× magnification field (0.74 mm^2) were counted simultaneously by two observers, and the average value for the five fields was calculated.

Statistical analysis

Key miRNAs verified by real-time qRT-PCR were analyzed using the public miRBase database (www.microrna.org), and the target proteins and pathways were analyzed using the public KEGG database (www.genome.jp). A normality test was performed on all data. Normally distributed data were compared by the t-test, a log-transformation was performed on other data to enable normal distribution, and abnormally distributed data were analyzed using the Mann–Whitney U test. Multiple groups were compared by ANOVA analysis, the Student–Newman–Keuls (SNK) test was used to compare the data in the groups, and the Pearson test was used for correlation analysis. The correlation analyses for clinicopathological subtypes and the various biological factors were examined by the X^2 test or t-test. For survival analysis, DFS was examined using the Kaplan–Meier curves. The log-rank test was used to compare survival differences between the groups. *P* values smaller than 0.05 were defined as statistically significant. Statistical analysis was performed using SPSS software (version 17.0).

Results

Differential distribution of miR-374a in tumors

MicroRNA array screening results (from 18 samples, 3 groups of six specimens) showed the expression of miR-374a ranging from low to high, ranked as HB<LA<LB<HA<Normal. According to the testing standard, which states that the fold-change value must be more than 2 or less than 0.5, the expression differences between the four tissue sample types were significant, showing as HB<HA<Normal, LA<LB<Normal, HB<LB<Normal, and LA<HA<Normal (Figure 2). The relative content of miR-374a in normal tissues was 0.32 ± 2.87, in LA was -7.11 ± 3.59, in LB was -3.95 ± 4.54, in HA was -3.31 ± 2.92, and in HB was -7.41 ± 3.99. The significant differences in the three groups were ranked as follows ($P<0.05$): HB<HA<Normal, LA<LB<Normal, HB<LB<Normal, and LA<HA<Normal (Figure 3A).

Target proteins as predicted using bioinformatics tools

The results of our bioinformatics analysis show that VEGF-A and VCAM-1 are the target proteins regulated by miR-374a (Table 2), and these targets play a key role

Table 2. Target Proteins and Regulatory MiRNAs

MicroRNA	Targets	Regulatory Sequences	mirSVR score	PhastCons score
miR-374a	VEGF-A	3' guGAAUA-GUCCA-ACAUAAUAUu 5' hsa-miR-374a 355:5' caUUUAUAUAUAUAUAUAUUAUAu 3' VEGFA	-1.2605	0.6989
VCAM-1		3' gugaAUAGUCCAAC---AUAAUAUu 5' hsa-miR-374a 335:5' cuagUGUU-GCUUGGACUAUUAUAa 3' VCAM1	-1.0780	0.6441

*Illustration: The predict-analysis was from the public data of net (www.microrna.org)

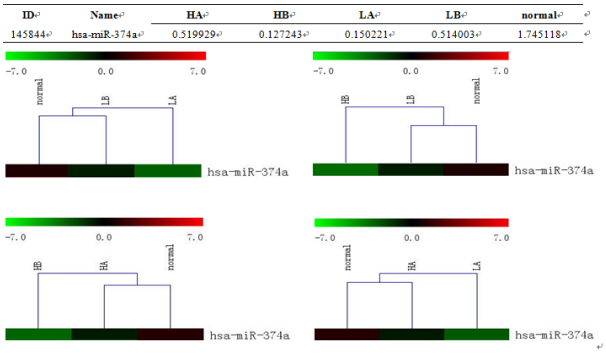

Figure 2. The Heat Map of the miR-374a

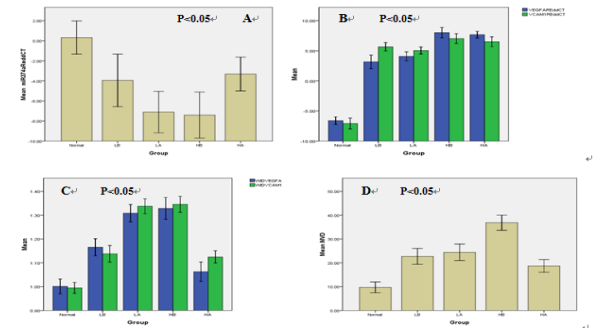

Figure 3. RT-qPCR Western-Blot, Immunohistochemistry

in the regulation of tumor angiogenesis.

Expression of VEGF-A and VCAM-1 (mRNA and protein) in breast tissue

The relative content of VEGF-A mRNA extracted from breast tissue in the Normal group was -6.60 ± 1.09, in LA was 4.08 ± 1.29, in LB was 3.18 ± 1.93, in HA was 7.69 ± 0.97, and in HB was 8.03 ± 1.48. The relative content of VCAM-1 mRNA extracted from breast tissue in the Normal group was -7.07 ± 1.57, in LA was 5.06 ± 1.03, in LB was 5.67 ± 1.23, in HA was 6.52 ± 1.43, and in HB was 7.04 ± 1.40. The significant differences in the two sets of three groups were ranked as follows (P<0.05): Normal<LA<HA and Normal<LB<HB (Figure 3B). The content of VEGF-A protein in the normal breast tissue group was 1.00±0.05, in LA group: 1.31±0.06, in LB: 1.17±0.06, in HA: 1.06 ± 0.07, and in HB: 1.33 ± 0.08. The content of VCAM-1 protein in breast tissue in the Normal group was 1.00 ± 0.04, in LA was 1.34 ± 0.05, in LB, 1.14 ± 0.06, in HA , 1.13 ± 0.04, and in HB, 1.35 ± 0.06. The significant differences between the four groups were ranked as follows (P<0.05): Normal<LB<HB; Normal<HA<LA; Normal<LB<LA and Normal<HA<HB (Figure 3C).

Expression of VEGF-A and VCAM-1 inversely correlates with miR-374a Expression in Breast Tissue

There was a significant negative correlation between

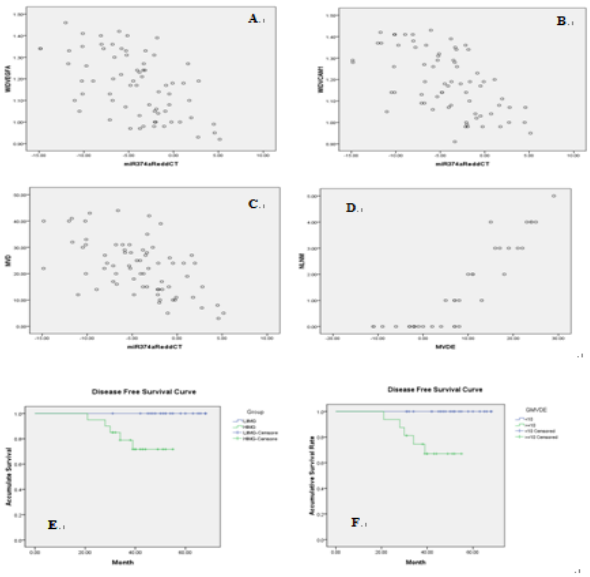

Figure 4. Scatter Correlation and Survival Analyses

the levels of miR-374a and VEGF-A protein extracted from breast tissue samples (Pearson correlation, r = -0.553, P<0.01) (Figure 4A) and between miR-374a and VCAM-1 protein levels (Pearson correlation, r = -0.578, P<0.01) (Figure 4B).

The distribution of MVD & correlation with the number of lymph node metastases

The mean breast tissue MVD in the Normal group was 9.45 ± 3.87, in LA, 25.40 ± 5.59, in LB, 23.90 ± 5.49, in HA, 18.95 ± 3.99, and in HB, 35.70 ± 5.81. The significant differences in the five groups were ranked as follows (P<0.05): Normal<HA<HB; Normal<LB<HB; Normal<LA<HB; Normal<HA<LA and Normal<HA<LB (Figure 3D). The difference in MVD was obtained by subtracting the value of MVD at the center from MVD at the edge of the tumor; the mean of differential MVD in LIMG group was -1.50 ± 5.35 and in HIMG, 16.25 ± 7.05 (Table 3). There was a significant negative correlation between MVD and the miR-374a (Pearson correlation, r = -0.567, P<0.01) (Figure 4C). There was a significant positive correlation between MVD and the number of metastatic lymph node (Pearson correlation, r = 0.912, P<0.01) (Figure 4D).

Profiles of patients & survival analysis

The distributions of characteristics between the two breast cancer groups are listed in Table 2; there were significant differences in DFS, median survival time, number of lymph node metastases, differences in MVD, chemotherapy, radiotherapy, and endocrine therapy between the groups (P<0.05). With a follow-up period from 28 to 68 months, the actuarial OS for

Table 3. Patients Parameters

Parameters	LIMG (n=20)	HIMG (n=20)	Statistics (t or X^2 or Wilcoxon)	*p*
Age(years)			0.552	0.584
Median	51.2	49.5		
Range	(37~71)	(25~66)		
Menopause			0.476	0.490
Yes	7	5		
No	13	15		
Quadrant			4.571	0.334
Areolar	1	5		
Outer upper	16	12		
Outer lower	1	0		
Inner lower	1	1		
Inner upper	1	2		
Operation			2.105	0.147
Mastectomy	18	20		
Tumorectomy	2	0		
Diameter	2.53±0.30	2.48±0.29	3.086	0.004
Number of LNM	0	2.65±1.27	63.865	0.000
Difference of MVD (Edge-Center)	-1.50±5.35	16.25±7.05	80.527	0.000
Overall Survival			2.105	0.147
Dead	0	2		
Survive	20 (100%)	18 (90%)		
Disease Free Survival			5.714	0.017
Cancer Progress	0	5		
None	20	15		
Local Recurrence	0	1		
Contralateral Tumor	0	2		
Hepatic Metastasis	0	1		
Multi-organ Metastasis	0	1		
Survive	20 (100%)	15 (75%)		
Median Survival Time (Month)	66	54	5.876	0.015
Chemotherapy			21.80	0.000
CMF	2	0		
CAF/AC	5	0		
CEF/EC	13	7		
TC/T	0	9		
TAC/AC-T	0	4		
Radiotherapy			32.727	0.000
No	20	2		
Yes	0	18		
Endocrine-therapy			40.000	0.000
No	0	20		
Yes	20	0		

*Illustration: There was significance difference between the LIMG and HIMG groups in diameter; DFS, median survival time, number of lymph nodes metastasis, difference of MVD, chemotherapy, radiotherapy, and endocrine-therapy; and no significance difference in other parameters

LIMG and HIMG was 100% and 90%, respectively, with no significant differences between the groups. The actuarial DFS in LIMG and HIMG was 100% and 75%, respectively, and the differences between these groups were significant (P = 0.017) (Table 3). The median survival time of patients in LIMG and HIMG was 66 and 54 months, respectively, and there were significant differences between the groups (P = 0.015) (Table 3), particularly between the disease-free survival curve (P = 0.013) (Figure 4E). If the discrepancy was less than 10microvessels, the distribution of MVD was considered uniform; if the discrepancy was greater than or equal to 10, the distribution was considered uneven. There was significant differences in the disease-free survival curve (P = 0.003) (Figure 4F).

Discussion

New vessel formation (angiogenesis) is an essential physiological process in embryonic development, normal growth, and tissue repair (Tassi et al., 2011). Angiogenesis is tightly regulated at the molecular level; however, this process is dysregulated in several pathological conditions such as cancer (Rapisarda et al., 2012). The cancer cell adaption for hypoxia is the main driving force of angiogenesis and evolution of heterogeneity (Crossin, 2012). A recent study has suggested that microRNAs mediate in metabolic stresses and angiogenesis during proliferation, invasion and metastasis of cancer (Patella et al., 2012). To determine how the key miRNAs are distributed and expressed in breast cancer tumors, examine possible differences in their expression and the relationship between these key miRNAs and angiogenesis, we chose to analyze the center and edge of breast cancer specimens. Specifically, microRNA array screening and verification tests were performed for the patients with different clinical prognoses. MiR-374a was unevenly distributed in breast tumors examined, as shown by the microRNA array analysis (Figure 2). The relative expression of miR-374a was lower in the center of the LIMG tumor than that at the edge; in the HIMG tumor, it was lower at the edge than that in the center, and lower in breast cancer tissues than in normal tissues (Figure 3A). Results presented by Võsa et al. indicate that low expression of miR-374a in early-stage non-small cell lung cancer is associated with poor patient survival (Võsa et al., 2011). Our results suggest that miR-374a might be involved in an anti-cancer response. According to our bioinformatics analysis, VEGF-A and VCAM-1 are the target proteins regulated by miR-374a (Table 2). VEGF-A and VCAM-1 mRNA levels were higher in the HIMG than in the LIMG, and they were also higher in HIMG and LIMG than in the Normal group; there were no differences between the expression levels at the edge and in the center of the tumor (Figure 3B). It is widely accepted that the higher the expression levels of VEGF-A mRNA, the poorer the breast cancer prognosis (Linderholm et al., 2000). VEGF-A is a pivotal driver of cancer angiogenesis and considered an important therapeutic target in the treatment of malignancy (Cao et al., 2012). The expression of VCAM-1 has been closely associated with oncogenesis, tumor angiogenesis and metastasis in cancer (Ding et al., 2003). We found that VEGF-A and VCAM-1protein levels were higher in the HIMG than in LIMG, and were higher in the LIMG than in the Normal group; the significant differences were ranked as LA>LB>Normal and HB>HA>Normal (Figure 3C). Our analysis showed that the expression of the miR-374a negatively correlated with the target protein (VEGF-A and VCAM-1) levels (Figure 4A, B). This negative correlation suggests that VEGF-A and VCAM-1 might be post-transcriptionally regulated by miR-374a; this conclusion should be confirmed by future experiments in vitro. Undoubtedly, the higher the expression of VEGF-A and VCAM-1, the more invasion and metastasis there will be. However, the patterns of the target protein distribution in the HIMG and LIMG tumors were completely opposite. The results of MVD analysis confirmed that VEGF-A and VCAM-1 induced angiogenesis in breast cancer, with different effects in LIMG and HIMG. The mean of MVD was higher in the HIMG than in LIMG, and it was higher in the LIMG than in the Normal group. The significant

differences were ranked as HB>HA>Normal; There was no difference between MVDs in LB and LA samples (Figure 3D). At the same time, there was a significant negative correlation between MVD and the miR-374a (Figure 4C). The prognostic value of MVD has remained controversial since its introduction twenty years ago: some initial studies have suggested that the MVD is a major independent prognostic factor for overall survival in invasive breast cancer (de Jong et al., 2000), but other studies have concluded that the MVD does not predict poor outcomes of invasive breast cancer (Kanjanapanjapol et al., 2007). Some recent research results have suggested that higher MVD is a favorable prognostic factor for early advanced breast cancer patients after adjuvant anthracycline-based chemotherapy (Biesaga et al., 2012). The authors of that study have speculated that differential distribution of MVD in tumors might be one of the reasons for different outcomes. The differential distribution of MVD demonstrated in our study suggests that the tumor is likely to be homogeneous in LIMG and heterogeneous in HIMG. Uniform distribution of the new vessels should be conductive to proliferation of cancer cells and the vessels concentrating at the edge of the tumor could favor invasion or metastasis. The analysis of vessel distribution in tumors might be useful for the prediction of metastasis and general disease prognosis. Our positive correlation between the MVD distribution within the tumors and the number of lymph node metastases gives some weight to this idea. To some extent, the difference between MVD at the tumor edge and in its center reflects heterogeneity of each tumor, particularly in terms of angiogenesis, and has a potential prognostic value. The stage II breast cancer was one of our inclusion criteria; LIMG belongs to luminal A clinicopathological subtype, HIMG belongs to Her2 overexpression subtype. In our study, the average DFS after four years was about 87.5% (35/40), slightly lower than in stage II breast cancer report of Kwong et al (Kwong et al., 2011). One of the reasons for the different DFS demonstrated for the two patient groups (LIMG and HIMG) in our study might be that we selected the patients with luminal A subtype, with the best prognosis, and the patients with Her2 overexpression subtype, with the poorest prognosis (Figure 4E). The differences might have been reinforced by the fact that, for various reasons, none of HIMG accepted target therapy. However, we believe that the more likely reasons for the large differences between prognoses for LIMG and HIMG were high complexity and diversity associated with grouping criteria. For example, HER-2 overexpression subtype breast cancers are known for their enhanced angiogenesis and low levels of hypoxia (Blackwell et al., 2004). In summary, it appears that one of the most important facets of the observed heterogeneity is the distribution of MVD. There was significant difference between the uniform and uneven groups in the disease-free survival curve, likely to affect the final prognosis and regulated by the mir-374a.

Acknowledgements

This research is supported by the Science and Technology Foundation of Liaoning Province, No. 2012225016. The author(s) declare that they have no competing interests.

References

Balsat C, Blacher S, Signolle N, et al (2011). Whole slide quantification of stromal lymphatic vessel distribution and peritumoral lymphatic vessel density in early invasive cervical cancer: a method description. *ISRN Obstet Gynecol*, **25**, 1-7.

Biesaga B, Niemiec J, Ziobro M (2012). Microvessel density and status of p53 protein as potential prognostic factors for adjuvant anthracycline chemotherapy in retrospective analysis of early breast cancer patients group. *Pathol Oncol Res*, **18**, 949-60.

Blackwell KL, Dewhirst MW, Liotcheva V, et al (2004). HER-2 gene amplification correlates with higher levels of angiogenesis and lower levels of hypoxia in primary breast tumors. *Clin Cancer Res*, **10**, 4083-8.

Cao Y, E G, Wang E, et al (2012). VEGF exerts an angiogenesis-independent function in cancer cells to promote their malignant progression. *Cancer Res*, **72**, 3912-8.

Caporali A, Emanueli C (2011). MicroRNA regulation in angiogenesis. *Vascul Pharmacol*, **55**, 79-86.

Crossin KL (2012). Oxygen levels and the regulation of cell adhesion in the nervous system: A control point for morphogenesis in development, disease and evolution? *Cell Adh Migr*, **6**, 49-58.

de Jong JS, van Diest PJ, Baak JP (2000). Hot spot microvessel density and the mitotic activity index are strong additional prognostic indicators in invasive breast cancer. *Histopathology*, **36**, 306-12.

Ding YB, Chen GY, Xia JG, et al (2003). Association of VCAM-1 overexpression with oncogenesis, tumor angiogenesis and metastasis of gastric carcinoma. *World J Gastroenterol*, **9**, 1409-14.

Jakóbisiak M, Lasek W, Gołab J (2003). Natural mechanisms protecting against cancer. *Immunol Lett*, **90**, 103-22.

Kanjanapanjapol S, Wongwaisayawan S, Phuwapraisirisan S, et al (2007). Prognostic significance of microvessel density in breast cancer of Thai women. *J Med Assoc Thai*, **90**, 282-90.

Kwong A, Mang OW, Wong CH, et al (2011). Breast cancer in Hong Kong, Southern China: the first population-based analysis of epidemiological characteristics, stage-specific, cancer-specific, and disease-free survival in breast cancer patients: 1997-2001. *Ann Surg Oncol*, **18**, 3072-8.

Linderholm B, Lindh B, Tavelin B, et al (2000). p53 and vascular-endothelial-growth-factor (VEGF) expression predicts outcome in 833 patients with primary breast carcinoma. *Int J Cancer*, **89**, 51-62.

Mackey JR, Kerbel RS, Gelmon KA, et al (2012). Controlling angiogenesis in breast cancer: A systematic review of anti-angiogenic trials. *Cancer Treat Rev,* **38**, 673-88.

Patella F, Rainaldi G (2012). MicroRNAs mediate metabolic stresses and angiogenesis. *Cell Mol Life Sci,* **69**, 1049-65.

Pritchard CC, Cheng HH, Tewari M (2012). MicroRNA profiling: approaches and considerations. *Nat Rev Genet*. **13**, 358-69.

Rapisarda A, Melillo G (2012). Role of the VEGF/VEGFR axis in cancer biology and therapy. *Adv Cancer Res*, **114**, 237-67.

Tassi E, McDonnell K, Gibby KA, et al (2011). Impact of fibroblast growth factor-binding protein-1 expression on angiogenesis and wound healing. *Am J Pathol*, **179**, 2220-32.

Võsa U, Vooder T, Kolde R, et al (2011). Identification of miR-374a as a prognostic marker for survival in patients with early-stage nonsmall cell lung cancer. *Genes Chromosomes Cancer*, **50**, 812-22.